

Supporting Information

Hayden et al. 10.1073/pnas.0812035106

SI Results

MUA Tracks Degrees of Task Engagement. We have argued that there is a strong functional correspondence between SUA and MUA in the CGp. To verify that the characteristic dependence on degrees of task vigilance in the functional response patterns we observed in single neurons (Fig. 4) is also characteristic of MUA, we performed the same analyses on the multiunits in our sample. We found that the average multiunit responses at sites in our sample showed the same default processing profile as single units. Specifically, we found that MUA was significantly greater on slow-reaction time trials (Student's t test, $P < 0.001$) than on fast-reaction time trials (Fig. S1A). We also found that MUA was significantly greater (Student's t test, $P < 0.05$) on error trials than on correct trials (Fig. S1B). Finally, we found that multiunit responses were significantly enhanced (Student's t test, $P < 0.01$) in the timeout condition (Fig. S1C). These data demonstrate that MUA in CGp shows the same processing profile as single neurons, as well as the population of neurons recorded. Finally, MUA tracks levels of task engagement in a continuous, rather than a discrete, manner (Fig. S1D), just as single units do (Fig. 5).

LIP Neurons Do Not Track Degrees of Task Engagement. We have argued that CGp and LIP play complementary roles in putative default processing. To verify that the functional default processing profile does not characterize LIP neurons, we examined the reaction time and error effects in the population of LIP neurons. In contrast to CGp neurons, LIP neurons showed a slight enhancement in activity on fast-reaction time trials (although this effect was not significant, Student's t test, $P = 0.08$; Fig. S2A). In addition, LIP neurons did not exhibit a significant enhancement for error trials (Fig. S2B). Instead, the firing rate of these neurons on error trials remained close to that observed on correct trials (Student's t test, $P = 0.6$). Interestingly, the firing rate on error trials was slightly enhanced during the early part of the response (although not significantly, $P = 0.4$) and suppressed later in the response (again, not significantly, $P = 0.5$).

Task-Related Suppression in CGp Is Observed for Both Subjects. To demonstrate that default effects were observed in the 2 subjects individually, and that the effects reported here were not limited to individual subjects, we separately analyzed SUA from the 2 subjects (monkeys N and D) individually. We found that both monkey N (Fig. S3A) and monkey D (Fig. S3B) exhibited clear default effects in CGp. In contrast, we found that neither monkey N (Fig. S3C) nor monkey D (Fig. S3D) exhibited such effects in LIP. Similar effects were observed in the working memory task.

The Relationship Between Reaction Time and Firing Rate (Example Cell). The relationship between reaction time and firing rate is shown for 1 cell in Fig. 4A. For this neuron, delay period firing rates (y axis) were higher on trials with slower reaction times (x axis). The significant positive correlation between these 2 variables ($r = 0.28$, $P < 0.005$) indicates that some of the variance in reaction times is explained by the variance in firing rates in CGp.

Free Viewing Does Not Evoke Changes in Firing Rate in CGp Neurons. To demonstrate that CGp neurons are not strongly driven by free-viewing eye movements, we analyzed saccade-aligned neuronal responses in a subset of neurons ($n = 52$) for which we

collected physiological data in the absence of any task demands. Natural saccades were made in the darkened experimental room outside the context of the task. Saccades typically lasted 60–90 ms (mean, 73.7 ms). Fixational periods between saccades typically lasted 180–240 ms (mean, 213.8 ms). For these neurons, we aligned neuronal responses to saccade onset, as determined by our eye monitoring system (Eyelink 1000, S.R. Research). We then compared neuronal responses in an 80-ms window beginning at the onset of saccade to those occurring in an 80-ms window beginning 160 ms later, during the fixational period. We observed modulations in firing rate for only 2 neurons (3.9% of neurons). Overall, firing rates during fixations and saccades did not differ ($P = 0.8$, Student's t test on modulations for individual neurons).

Supplemental Methods. All procedures were approved by the Duke University Institutional Animal Care and Use Committee and were designed and conducted in compliance with the Public Health Service's Guide for the Care and Use of Animals. Two male rhesus monkeys (*Macaca mulatta*) served as subjects. A small prosthesis was implanted in both animals by using standard surgical techniques. Four weeks later, animals were habituated to training conditions and trained to perform oculomotor tasks for a liquid reward. A second surgical procedure was then performed to place a stainless steel chamber (Crist Instruments) over the CGp (in one monkey) and over the LIP cortex (in the other monkey). In both cases, one recording location was approached through a standard vertical recording grid (CGp for monkey N and LIP for monkey D), whereas the other area was approached by an angled grid (LIP for monkey N and CGp for monkey D). Animals received analgesics and antibiotics after all surgeries. Throughout both behavioral and physiological recording sessions, the chamber was kept sterile with regular antibiotic washes and sealed with sterile caps.

Monkeys were placed on controlled access to fluid outside of experimental sessions. Horizontal and vertical eye positions were sampled at 1,000 Hz by an infrared eye-monitoring camera system (SR Research). Stimuli were controlled by a computer running Matlab (Mathworks) with Psychtoolbox and Eyelink Toolbox (1, 2). Visual stimuli were small, colored squares on a computer monitor placed directly in front of the animal and centered on his eyes. A standard solenoid valve controlled the duration of juice delivery. Reward volume was 0.2 mL in all cases.

In the attentive and working memory tasks, the trial began with the appearance of a small, yellow, fixation square. The square then changed color to indicate the nature of the task (red for memory, green for attentive, and remaining yellow for timeout). The square remained on for 4 seconds (monkey N) or 3 seconds (monkey D) and was then extinguished, signaling a saccade. In the working memory task, an eccentric cue appeared after 2 seconds of fixation (monkey N) or 1 second (monkey D). The cue remained illuminated for 1 second and then disappeared. In the attentive task, an eccentric cue appeared at the end of the delay, and the monkey was rewarded for shifting its gaze to it as quickly as possible. In the working memory task, no eccentric cue appeared, and the monkey had to shift its gaze to the remembered location. A fluid reward was given following successful completion of either task. In the timeout condition, no other stimuli appeared, and no reward was given. ITIs were fixed at 3 seconds in all cases.

In monkey N, we approached CGp through a standard re-

cording grid normal to the horizontal plane, and we approached LIP through a 30-degree grid angled caudolaterally. In monkey D, we approached LIP through a standard recording grid normal to the horizontal plane, and we approached CGp through a 30-degree grid angled rostromedially. LIP was identified stereotactically; localization was confirmed by characteristic saccade-related MUA with strong contralateral tuning. CGp was identified by its low firing rates and distinguished from somatosensory cortex by a lack of tactile responsiveness. Following some recording sessions, we confirmed the location of the electrode by using a hand-help digital ultrasound device (Sonosite 180, Sonosite Inc.) placed against the recording chamber.

Statistical Methods. PSTHs were constructed by aligning spike rasters to trial events and averaging firing rates across multiple trials. Firing rates were then combined in 16.67-ms bins, and then the resulting curve was smoothed by using a 20-bin running boxcar. In the PSTHs, data were aligned to the onset of the saccade at the beginning of the trial or to the saccade that ended the trial to account for different trial durations used for the 2 animals. Data from error trials, including those on which eyes were closed for more than 200 ms, were excluded from analyses. By excluding data from trials on which eyes were closed, we have eliminated the possible confound that monkeys slept during certain trials.

Statistical comparisons were performed on binned, but unsmoothed, firing rates of single neurons. To compare firing rates across trials, for each single neuron, a Student's *t* test was performed on individual trials; to compare firing rates across neurons, a Student's *t* test was performed on the average rates computed for each individual neuron. Although neuronal firing rates tend to occur in a Poisson or super-Poisson distribution, these distributions become much more Gaussian as bin sizes grow longer. Because the bin sizes in the present study all lasted multiple seconds, we are confident that distributions of firing rates do not strongly violate the assumption of Gaussianity

required by the *t* test. Nonetheless, we performed a nonparametric hypothesis test in all cases (a bootstrap *t* test with 1,000 reshuffled estimates of the mean) and did not find qualitatively different estimates of the *P* value in any case.

In all cases, firing rates were compared in a 3-second window beginning half a second after fixation was acquired (for monkey N) or a 2-second window beginning half a second after fixation was acquired (for monkey D). In the no-task condition, responses were aligned to the time that the fixation cue would have appeared. We calculated the total number of spikes during this epoch in each trial and compared the distributions of spikes for all trials of each type in the comparison by using a Student's *t* test. We confirmed all analyses with nonparametric tests and found nearly identical results in all cases.

The firing rates of neurons at a multiunit site depend mostly on the threshold set by the experimenter when the data were collected. Because no systematic effort was made to control this parameter, the actual firing rate of the multiunits was therefore statistically meaningless. We therefore normalized all MUA firing rates to have the same mean and performed all analyses on the normalized responses. Local field potentials were analyzed in 2 ways. Our primary analysis method consisted of a multitaper spectral analysis as performed by a freely available Matlab package designed for analysis of neural data (Chronux). Analysis was preceded by notch-filtering any 60-Hz line noise and subtracting the ITI bias in each sample. These analyses were confirmed by using a standard Matlab implementation of the fast Fourier transform. In all cases, results using the 2 methods were qualitatively similar. In general, significance was estimated by using standard Student's *t* tests. Specifically, each LFP time series was transformed to the spectral domain, then log transformed, and then the LFPs in the 2 conditions were subtracted. This difference was calculated for each neuron, and all statistics were performed on the population of differences obtained for all of the recordings in the population. As with firing rate comparisons, tests were 2-tailed in all cases.

1. Cornelissen FW, Peters E, Palmer J (2002) The eyelink toolbox: Eye tracking with MATLAB and the psychophysics toolbox. *Behavior Research Methods, Instruments & Computers* 34:613–617.

2. Brainard DH (1997) The psychophysics toolbox. *Spat Vis* 10:433–436.

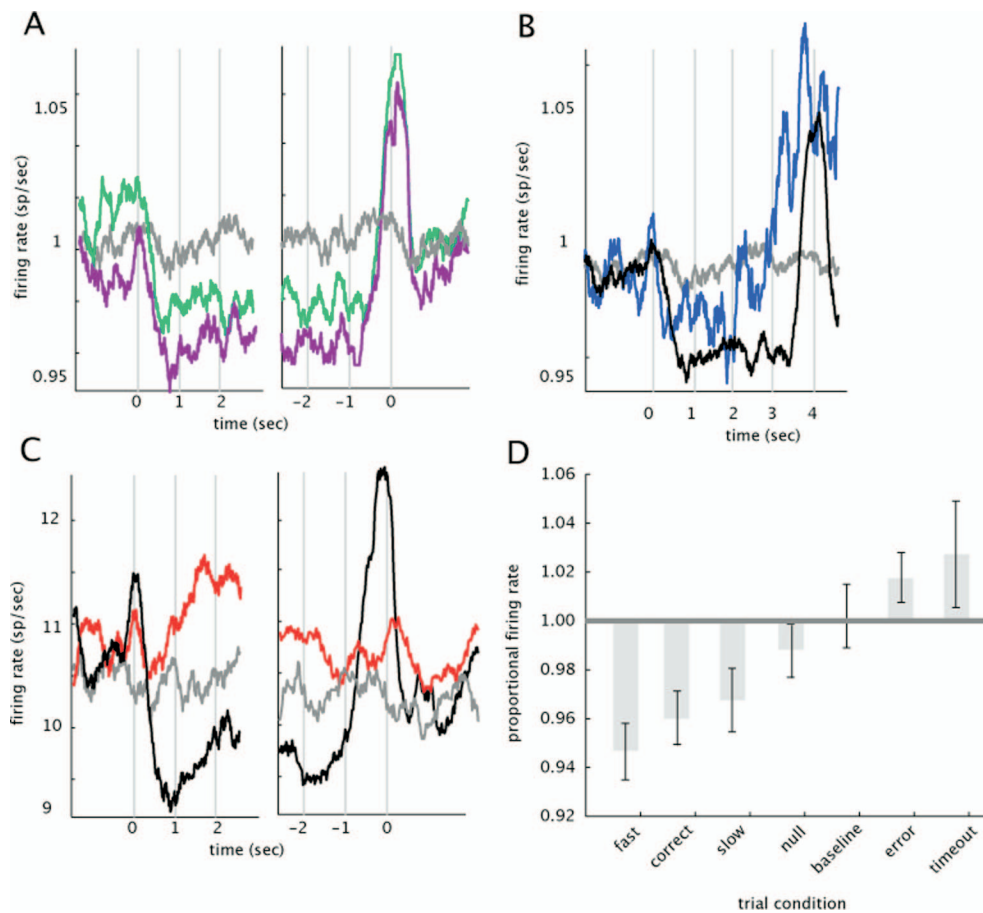


Fig. S1. Activity of population MUA in CGp shows the default processing profile. (A) PSTHs aligned on fixation and showing average MUA at all CGp sites on trials with slow (reaction time > median; green line) and fast (reaction time < median; purple line) reaction times. MUA was lower before trials on which subsequent reaction times were faster. (B) PSTHs showing average MUA in CGp on error (blue line) and correct (black line) trials of attentive task, as well as in rest condition (gray line). PSTHs on error trials were truncated 500 ms before error occurred. Difference in responses emerged before trial began. (C) PSTHs showing average multiunit response on timeout trials. When cue indicated that trial would not begin immediately (timeout), MUA was significantly enhanced. (D) Bar graph showing average normalized firing rate of MUA in each of the conditions outlined above. sp/sec indicates spikes per second.

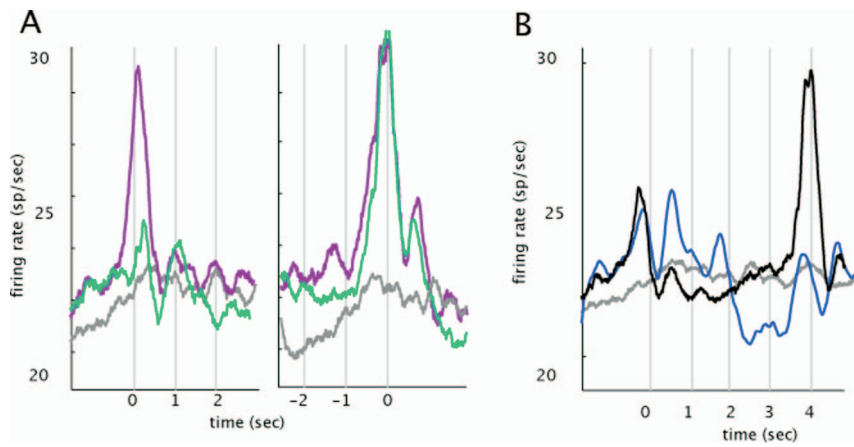


Fig. S2. Neuronal activity in LIP does not track with task engagement. (A) PSTHs aligned on fixation and showing average firing rates of population of LIP neurons ($n = 54$) on trials with slow (reaction time $>$ median; green line) and fast (reaction time $<$ median; purple line) saccade reaction times. Neuronal activity did not vary significantly on reaction time. (B) PSTHs plotting average firing rate of population activity in LIP on error (blue line) and correct (black line) attentive trials, as well as in the rest condition (gray line). Responses on error trials were truncated 500 ms before errors occurred.

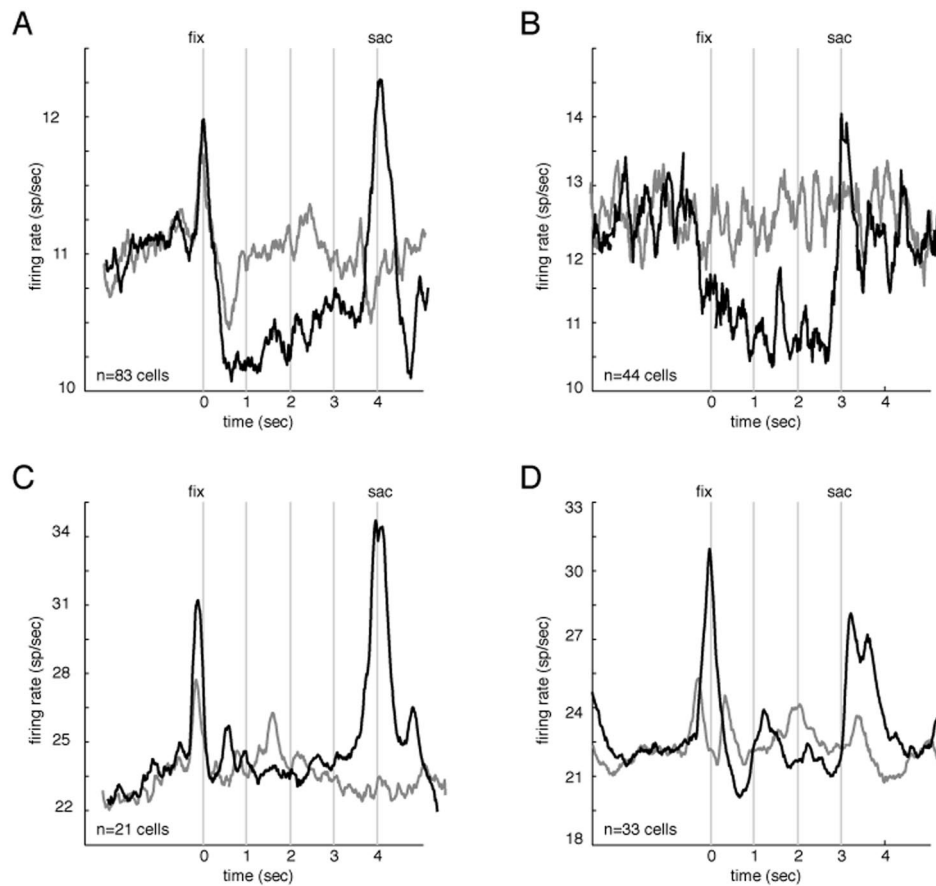


Fig. S3. PSTHs for the subjects individually in baseline and attentive conditions. (A and B) PSTHs representing population activity of CGp neurons for monkeys N and D, respectively. These figures indicate that functional properties of CGp neurons are consistent across subjects. Note that 3-second trials were used for monkey D, whereas 4-second trials were used for monkey N. (C and D) PSTHs representing population activity of LIP neurons for monkeys N and D, respectively. Note that 3-second trials were used for monkey D, whereas 4-second trials were used for monkey N.

Table S1. Reductions in CGp firing rates relative to ITI for each monkey

	Monkey N			Monkey D		
	Firing rate reduction, spikes per second	Percent reduction	P value	Firing rate reduction, spikes per second	Percent reduction	P value
Baseline condition	-0.10	-0.9	>0.05	-0.02	-0.16	>0.05
Attentive task	-0.62	-5.6	<0.001	-1.2	-9.8	<0.001
Working memory task	-0.82	-7.4	<0.001	-1.4	-11.4	<0.001
Timeout condition	0.8	7.6	<0.01	0.65	7.59	<0.05

Columns provide absolute change in firing rate, percent change in firing rate, and *P* value for change for monkeys N and D individually. First row shows average firing rate reduction for the baseline condition. Second row shows average firing rate reduction for the attentive task. Third row shows average firing rate reduction for the working memory task. Fourth row shows average firing rate enhancement for timeout condition. Firing rates were collected during a long epoch beginning 500 ms after fixation and ending 500 ms before the end of the trial.

Table S2. Changes in CGp correlate with behavior in individual monkeys

	Monkey N			Monkey D		
	Firing rate, spikes per second	Percent	P value	Firing rate, spikes per second	Percent	P value
Reaction time effect	0.75	6.7	<0.001	0.6	4.9	<0.001
Error effect	1.1	9.9	<0.001	1.4	11.4	<0.001

Columns provide absolute change in firing rate, percent change in firing rate, and *P* value for change for monkeys N and D individually. First row shows average difference in firing rate for slow- and fast-reaction time trials. Second row shows average firing rate enhancement on error trials. Firing rates for reaction time and timeout were collected during a long epoch beginning 500 ms after fixation and ending 500 ms before the end of the trial. Firing rates for error effect were collected during trial until 500 ms before the error occurred.

Table S3. Changes in LIP firing rates for each monkey in each task

	Monkey N			Monkey D		
	Firing rate increase, spikes per second	Percent increase	P value	Firing rate increase, spikes per second	Percent increase	P value
Baseline condition	0.7	3.0	<0.05	0.79	3.6	<0.05
Attentive task	1.41	6.0	<0.05	0.42	1.9	<0.05
Working memory task	1.48	6.2	<0.05	0.9	4.0	<0.05

Columns provide absolute change in firing rate, percent change in firing rate, and *P* value for change for monkeys N and D individually. First row shows average firing rate reduction for the baseline condition. Second row shows average firing rate reduction for the attentive task. Third row shows average firing rate reduction for the working memory task. Firing rates were collected during a long epoch beginning 500 ms after fixation and ending 500 ms before the end of the trial.

Table S4. Changes in LIP do not correlate with behavior in individual monkeys

	Monkey N			Monkey D		
	Firing rate, spikes per second	Percent	P value	Firing rate, spikes per second	Percent	P value
Reaction time effect	0.33	1.4	>0.05	0.31	1.3	>0.05
Error effect	0.24	1.4	>0.05	0.87	3.9	>0.05

Columns provide absolute change in firing rate, percent change in firing rate, and *P* value for change for monkeys N and D individually. First row shows average difference in firing rate for slow- and fast-reaction time trials. Second row shows average firing rate enhancement on error trials. Third row shows average firing rate enhancement on timeout trials. Firing rates for reaction time and timeout were collected during a long epoch beginning 500 ms after fixation and ending 500 ms before the end of the trial. Firing rates for error effect were collected during the trial until 500 ms before the error occurred.

Table S5. Percentage of neurons exhibiting a significant correlation between firing rate and reaction time

	Positive, %	No effect, %	Negative, %
CGp	38	51	11
LIP	6	88	6

Increased firing rates were associated with slower reaction times in a significant fraction of neurons in CGp but not LIP.